

Thermal Model Calculations for Hot and Dense Hadronic Matter Using van der Waals Type Equation of State

Rameez Ahmad Parra^a, Saeed Uddin^a, Waseem Bashir^{a,b} and Inam-ul Bashir^{a,c}

^a Department of Physics, Jamia Millia Islamia, New Delhi, India

^b Department of Physics, Govt. Degree College, Budgam, J&K, India

^c Govt. Boys Higher Secondary School, Tral, J&K, India

Abstract

We incorporate the Van der Waals interaction in the hadron resonance gas model to obtain the particle ratios $\frac{\bar{N}}{N}, \frac{\bar{\Lambda}}{\Lambda}, \frac{\bar{\Xi}}{\Xi}, \frac{\Omega^+}{\Omega^-}$ & $\frac{\kappa^-}{\kappa^+}$ and study their dependence on temperature and baryon chemical potential (μ_B). These results on particle ratios are compared with the point-like hadron case. It is found that the particle ratios get significantly modified in the case of van der Waals interactions. In the van der Waals type equation of state (EoS) both the attractive and repulsive parts of interactions are taken into account. In some previous works the attractive and repulsive parameters were fixed as ($a = 329 - 1250$ MeVfm 3) and ($b = 3.42 - 5.75$ fm 3), respectively. These parameters were fixed from the ground state properties of nuclear matter. However, by using a fixed value of the parameter "a" we don't get baryon (B) antibaryon (\bar{B}) symmetry for $\mu_B = 0$. This results in a situation where antibaryon/baryon ratio becomes greater than unity, which is unphysical. In order to solve this discrepancy, we make the attractive parameter "a" function of temperature such that it gives physically acceptable results.

Key Words: HRG Model, Particle Ratios, Baryon Antibaryon Symmetry, van der Waals Interactions

1. Introduction

Hadronic yields are an important tool to understand the multi-particle production phenomenon in the ultra-relativistic nuclear collisions. The study of the various hadronic species multiplicity in the nuclear collisions at ultra-relativistic energies allows us to understand the final stage property of the hot and dense hadronic matter produced in such collisions which may have attained a reasonably high degree of thermal and chemical equilibrium.

After the initial collision, the hot and highly dense secondary partonic matter produced (consisting of quarks and gluons) is in a pre-equilibrium state. However, due to multiple collisions among these secondary partons a reasonably high degree of thermal and chemical equilibrium is achieved leading to the possible formation of quark gluon plasma (QGP) state. This is then followed by a QGP-hadron gas mixed state and then finally the system goes into a state of hot and dense interacting hadrons. As the secondary collisions among the hadrons continue hence a high degree of thermo-chemical equilibrium in the hadronic phase may be attained. As the system expands, cools and gets diluted the mean free path of the various hadronic species becomes comparable with the system size and consequently the hadrons no longer strongly interact with each other and a thermo-chemical “freeze-out” occurs. The final freeze-out state of the hot and dense hadronic matter has often been described in the framework of thermal hadronic resonance gas models.

The ideal hadron resonance gas model of point-like non-interacting particles does not reproduce the ground state properties of the nuclear matter. Besides no reasonable quark hadron phase transition in the theoretical models is obtained with sufficiently large number of degrees of freedom [1-4] because at sufficiently high temperature (T) a large number of point-like hadronic resonances can be thermally excited (without repulsive interaction). Consequently, in a thermodynamical model assuming a first order quark-hadron phase transition with a large number of hadronic degrees of freedom, the hadronic pressure becomes larger than quark gluon plasma (QGP) pressure and the system reverts to the HRG (hadron resonance gas) phase at sufficiently high temperatures. This contradicts the lattice quantum chromodynamics (LQCD) predictions where the phase transition occurs at the critical temperature around 160-180 MeV for vanishing net baryon number and the system remains in the QGP phase for further higher temperatures. In the thermal model approach this problem can be solved by considering the repulsive interaction between baryon or antibaryons also leading to an excluded volume type effect. However, in a more realistic approach both the attractive and repulsive interactions should be taken into account. The repulsive interaction is found to be proportional to number

density (n) and which vanishes for $n \cong 0$. Such kind of equation of state (EoS) may be used as an input for the hydro-dynamical model of nuclear collisions [5-7].

In the present work, we use grand canonical ensemble (GCE) partition function approach to explain the properties of baryonic matter. This is because of the fact that the canonical ensemble pressure doesn't provide a comprehensive thermodynamical picture of the system as the specification of the variables like volume (V), temperature (T) and the number of particles (N) are not the accepted variables for pressure function and the number of hadrons of a given type is usually not conserved in the real systems. The GCE formulation provides a very suitable framework for incorporating the attractive and repulsive interactions into the multi-component hadron gas. The GCE formulation can be effectively used to calculate abundances of various particles and their ratios. The repulsive part is incorporated through the excluded volume effect in the hadron resonance gas (HRG) model and is generally known as EV-HRG model of heavy ion collisions [8-11] and the attractive parameter is introduced by multiplying partition function with some exponential factor containing attractive potential. There are however other ways also of modelling the attractive and repulsive interactions such as Walecka model and its generalizations [12-16]. In van der Waals model strength of repulsion is proportional to the total particle density and is finite at zero baryon chemical potential ($\mu_B = 0$), on the other hand in Walecka model, the strength of repulsion is proportional to the net particle density and hence vanishes at ($\mu_B = 0$). This is therefore a significant advantage of van der Waals approach over Walecka model. We have arranged this article as follows. In section 2, we have derived the expressions for effective baryon chemical potential (μ_B^*) and the modified number density (n) using grand partition function formulation with repulsive as well as attractive interactions. In section 3, we have discussed the results and in section 4, we summarise our results and make conclusion.

2. Model

The GCE formulation of equation of state (EoS) of hadronic matter is presented in this section. We have taken both the attractive and repulsive interactions among the baryons. The van der Waals equation of state (EoS) governing the behaviour of baryonic matter can be derived from the grand partition function. The ideal (i.e. for point-like hadrons) grand partition function is given by:

$$Z(T, \mu, V) = \sum_{N=0}^{\infty} e^{\mu N / T} Z(T, N, V) \quad (1)$$

For simplicity we have used $\mu_B = \mu$ in the remaining part of this section.

By introducing the interactions in the ideal grand partition function in equation (1) can be rewritten as:

$$Z^{int}(T, \mu, V) = \sum_{N=0}^{\infty} e^{\frac{\mu N}{T}} \times Z(T, N, V - V_0 N) e^{-\bar{U}/T} \quad (2a)$$

Where, $V - V_0 N$ is the excluded volume, which arises out of the repulsive interaction and the attractive interaction is incorporated by introducing the factor $e^{-\bar{U}/T}$ in the grand partition function, \bar{U} represents the average attractive interaction energy assuming uniform density, $n=N/V$. The average attractive interaction energy can be written as:

$$\bar{U} = \frac{1}{2} \sum_{i,j} V_{att}(\vec{r}_i - \vec{r}_j) \quad (2b)$$

Where $V_{att}(\vec{r}_i - \vec{r}_j)$ is the average interaction energy of two particles (it does not matter which two, as they are all identical), it depends on the coordinates of two particles. At any given instant of time we can consider only one pair of particles which is sufficient [6]. Therefore the total interaction energy can be obtained by summation over all the particles, equation (2b) takes the form (for large n):

$$\bar{U} \approx \frac{1}{2} n^2 V \int d^3 \vec{r} V_{att}(\vec{r})$$

Where, \vec{r} is the relative coordinate. We can thus write:

$$\bar{U} = \frac{N^2 a}{V} \quad (3)$$

We have defined, $a = \int 2\pi r^2 dr V_{att}(\vec{r})$, where "a" represents the attractive interaction parameter. Equation (2) can be rewritten as:

$$Z^{int}(T, \mu, V) = \sum_{N=0}^{\infty} e^{\frac{\mu N}{T}} \times Z(T, N, V - V_0 N) e^{-\frac{N^2 a}{V T}} \quad (4)$$

We take the Laplace transform of equation (4) in order to indentify the pressure function by considering the extreme right hand singularity. For more detail on this approach one may refer to Rischke et al [2].

$$Z^{int}(T, \mu, \zeta) = \int e^{-\zeta V} Z^{int}(T, \mu, V) dV \quad (5)$$

Using equation (4) in equation (5), we get:

$$Z^{int}(T, \mu, \zeta) = \int e^{-\zeta V} dV \sum_{N=0}^{\infty} e^{\frac{\mu N}{T}} \times Z(T, N, V - V_0 N) e^{-\frac{N^2 a}{V T}} \quad (6)$$

The equation (6) can be rewritten as:

$$Z^{int}(T, \mu, \zeta) = \int e^{-\zeta V} dV Z^{excl}(T, \mu, V) \times e^{-\frac{N^2 a}{VT}} \quad (7)$$

where,

$$Z^{excl}(T, \mu, V) = \sum_{N=0}^{\infty} e^{\frac{\mu N}{T}} Z(T, N, V - V_0 N)$$

From equation (7), we can write:

$$Z^{int}(T, \mu, \zeta) = \int e^{-V \left(\zeta - \frac{\ln Z^{excl}(T, \mu, V)}{V} + \frac{N^2 a}{V^2 T} \right)} dV \quad (8)$$

The finiteness of the above integral requires that in the infinite volume limit, we must have a singular point given by the following condition:

$$\zeta - \frac{\ln Z^{excl}(T, \mu, V)}{V} + \frac{N^2 a}{V^2 T} = 0 \quad (9)$$

This gives:

$$\zeta = \frac{1}{T} \{ p^{excl}(T, \mu, V) - N^2 a / V^2 \} \quad (10)$$

Where $p^{excl}(T, \mu, V) = \lim_{V \rightarrow \infty} \frac{T \ln Z^{excl}(T, \mu, V)}{V}$

As $\xi T = p^{int}$, Therefore the final expression for pressure comes out to be:

$$p^{int}(T, \mu, V) = \frac{nT}{1-bn} - an^2 \quad (11)$$

Where, $p^{excl}(T, \mu, V) = \frac{nT}{1-bn}$

The number density can be obtained from partial derivative of pressure function with respect to chemical potential:

$$n = \left. \frac{\partial p^{int}}{\partial \mu} \right|_T = \left. \frac{\partial p^{int}}{\partial n} \right|_T \times \left. \frac{\partial n}{\partial \mu} \right|_T \quad (12)$$

Using equation (11) in equation (12), we get:

$$n = \left. \frac{\partial}{\partial n} \left(\frac{nT}{1-bn} - an^2 \right) \frac{\partial n}{\partial \mu} \right|_T \quad (13)$$

From equation (13), we can write:

$$n = \left(\frac{T}{(1-bn)^2} - 2an \right) \left. \frac{\partial n}{\partial \mu} \right|_T$$

or, $\mu = \int \frac{Tdn}{n(1-bn)^2} - \int 2adn + C \quad (14)$

This finally gives:

$$\mu = T \log \left(\frac{n}{1-bn} \right) + \frac{T}{1-bn} - 2an + C \quad (15a)$$

The value of constant of integration is to be determined at $a=b=0$, $\mu = \mu^{id}$, $n = n^{id}$. The value of C comes out to be:

$$C = T \log \left(\frac{n^{id}}{\phi} \right) - T \log(n^{id}) - T$$

The equation (15a) can be rewritten as:

$$\mu = T \log \left\{ \frac{n}{(1-bn)\phi} \right\} + \frac{bnT}{1-bn} - 2an \quad (15b)$$

We define,

$$\mu^* = T \log \left\{ \frac{n}{(1-bn)\phi} \right\} \quad (15c)$$

where

$$\phi = n^{id}(T, \mu^*) e^{-\mu^*/T}$$

Equation (15b), takes the form:

$$\mu^* = \mu - \frac{bnT}{1-bn} + 2an \quad (16)$$

Equation (16), defines the "effective" chemical potential (μ^*) for single hadronic species.

From equation (15c), we can write:

$$\frac{\mu^*}{T} = \log \left\{ \frac{n}{(1-bn)\phi} \right\} \quad (17)$$

Using $n^{id}(T, \mu^*) = e^{\mu^*/T} \phi$ and $\phi = n^{id}(T, \mu^*) e^{-\mu^*/T}$ in equation (17), we get:

$$n = \frac{n^{id}(T, \mu^*)}{1 + bn^{id}(T, \mu^*)} \quad (18)$$

For multi-component hadronic species (say j^{th}), the generalization of equation (16) gives:

$$\mu_j^* = \mu_j - \frac{b_j n_j T}{1 - \sum_i b_i n_i} + 2a n_j$$

which finally yields:

$$n_j = \frac{n_j^{id}(T, \mu^*)}{1 + \sum_j b_j n_j^{id}(T, \mu^*)} \quad (19)$$

The equation (19) is the modified number density (n_j) of the j^{th} type hadronic specie for the interacting baryonic matter using van der Waals interactions, where " b " is the excluded volume parameter ($b_j = \frac{16}{3} \pi r_j^3$), r_j is the radius of the j^{th} hadronic species. It is to be stressed here that this approach provides results which are *thermodynamically consistent*. The same procedure can be applied for the anti-baryonic matter by changing ($\mu^* \rightarrow -\mu^*$). We have extended this model to

baryon octet, omega and Kaons, which were not discussed in most of the previous works except for the case of nucleons [17,22]. In the following we discuss the results.

Here it is also important to define the chemical potentials of various hadrons. We follow the following standard procedure.

For each light valence (u, d) quark in a given hadronic specie we assign it a chemical potential μ_q , with $\mu_q = \mu_B/3$ where μ_B is the baryon chemical potential. Hence for a hadron with N_q number of light valence quarks the corresponding chemical potential will be $N_q\mu_q$. Similarly we assign it an additional chemical potential $N_s\mu_s$, where μ_s is the strange quark chemical potential and N_s is the number of valence strange quarks in the given hadronic specie. Consequently the chemical potential of a given j^{th} hadronic specie will be $\mu^j = N_q^j\mu_q + N_s^j\mu_s$. If a hadron contains N_q number of valence light *antiquarks* and N_s number of valence *antistrange* quarks its chemical potential be written as $\mu_j = -N_q\mu_q - N_s\mu_s$. For example this gives for Lambda (having 2 light quarks and 1 strange quark) $\mu_\Lambda = 2\mu_q + \mu_s$. For Kaon which contains a light quark and a strange antiquark we similarly get $\mu_K = \mu_q - \mu_s$. This procedure can be similarly applied to define the chemical potentials of all other hadrons (mesons, baryons and antibaryons). The overall strangeness conservation criteria then requires that the total strangeness content of the system must be equal to the total antistrange content of the system. This is used to fix the value of the strange chemical potential μ_s for a given value of μ_B (or μ) and T.

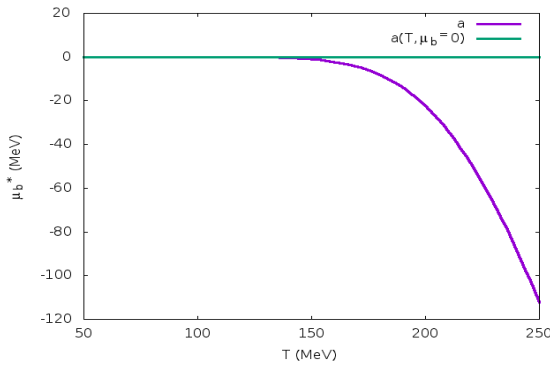
3. Results and Discussion

In figure 1(a) we have shown the variation of the “effective” baryon chemical potential (μ_B^*) with temperature at zero baryon chemical potential ($\mu_B = 0$). In many earlier works employing different model approaches, different but fixed, values of the parameter a have been used (329-1250 MeV-fm³) [17-22]. In this case, i.e. figure 1(a), we have used a constant value of the attractive parameter ($a=329$ Mev-fm³). This value is obtained from the ground state properties of nuclear matter. We find that at temperatures larger than 150 MeV the effective baryon chemical potential (μ_B^*) becomes (non zero) negative. This clearly implies that baryon (B) anti-baryon (\bar{B}) symmetry of the system is not maintained at $\mu_B = 0$. As a result the antibaryon to baryon ratio, (\bar{B}/B) , becomes greater than unity resulting in an unphysical situation where baryon-antibaryon symmetry is lost. In order to overcome this discrepancy we have imposed the criteria that when baryon chemical potential (*i.e.* μ_B) becomes zero the “effective” baryon chemical

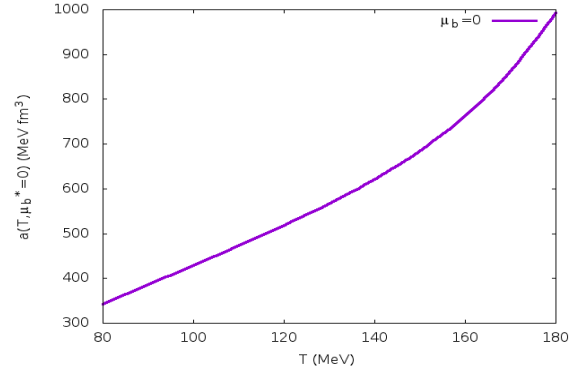
potential (μ_B^*) also becomes zero at all temperatures. This condition yields the following relation:

$$a(T, \mu_B = 0) = \frac{bT}{2(1-bn)} \quad (20)$$

This condition makes the attractive model parameter a temperature dependent. In figure 1(b) we have shown variation of attractive parameter $a(T, \mu_B = 0)$ as a function of temperature.



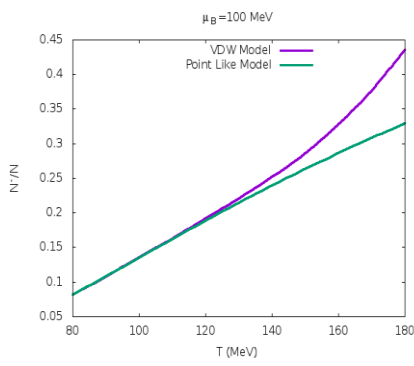
(Fig. 1a)



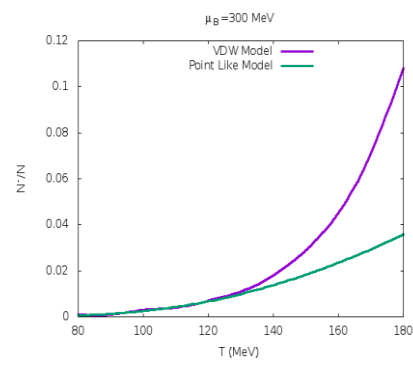
(Fig. 1b)

Fig 1: Variation of effective chemical potential (μ_B^*) shown in Fig. 1a and attractive parameter a shown in Fig. 1b, as a function of temperature.

In figures 2(a), 2(b) and 2(c), we have plotted the variation of anti-nucleon to nucleon ratio ($\frac{\bar{N}}{N}$) with temperature at fixed baryon chemical potentials, $\mu_B = 100$ MeV, 300 MeV and 500 MeV, respectively. We have compared this ratio obtained from our calculation, using van der Waals (VDW) type EoS, with case of the point-like hadrons. In van der Waals (VDW) type EoS we see an enhancement in the particle ratios as compared those obtained in the point-like hadrons case at higher temperatures. The variation becomes more significant for higher values of μ_B where it shows a rapidly increasing trend.



(Fig. 2 a)



(Fig. 2b)

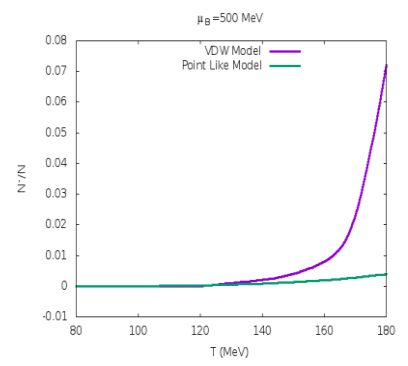


(Fig. 2c)

Fig 2: Variation of particle ratios ($\frac{\bar{N}}{N}$) with temperature at fixed baryon chemical potentials, $\mu_B = 100$ MeV, 300 MeV and 500 MeV.

We have also obtained the antistrange to strange hyperon ratios using our calculations. This will help us understand the extent of the effect of the modification in the values of the “effective” baryon as well as strange chemical potentials i.e. μ_B^* and μ_s^* on (anti)strange particles. With this purpose we have calculated the singly (anti)strange particles ratio. In the figures 3(a), 3(b) and 3(c) we have shown the variation of antilambda to lambda, $(\bar{\Lambda})/\Lambda$, ratio with temperature at different values of fixed baryon chemical potential, i.e. $\mu_B = 100$ MeV, 300 MeV and 500 MeV, respectively. We have also compared these ratios obtained in van der Waals (VDW) type EoS with those obtained for the point-like hadrons cases. It is found that particle ratios get modified at higher temperatures and chemical potentials using van der Waals (VDW) type EoS where it shows significant enhancement.

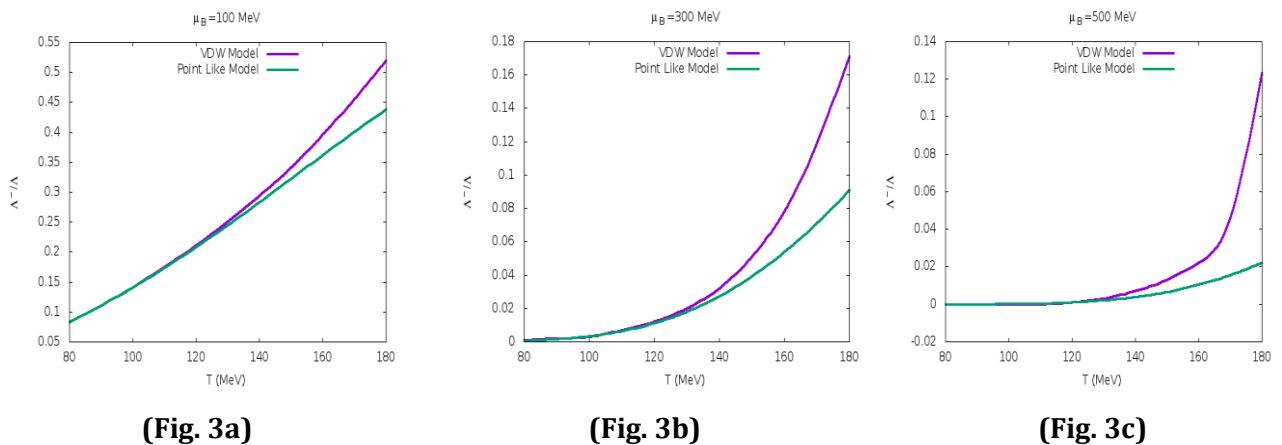


Fig 3: Variation of particle ratio $(\bar{\Lambda})/\Lambda$ with temperature at fixed baryon chemical potential $\mu_B = 100$ MeV (Fig. 3a), 300 MeV (Fig. 3b) and 500 MeV (Fig. 3c).

In figures 4(a), 4(b) and 4(c), show the variation of the doubly (anti)strange particle ratios, i.e. anticascade to cascade, $(\bar{\Xi})/\Xi$, ratio with temperature at fixed baryon chemical potential $\mu_B = 100$ MeV, 300 MeV and 500 MeV, respectively. In this case we notice that when we use van der Waals (VDW) EoS the modification (enhancement) in the $(\bar{\Xi})/\Xi$ ratio compared to the point like hadron case is small, while it is significant in the cases of \bar{N}/N and $\bar{\Lambda}/\Lambda$. This is because of the fact that cascade contains two strange quarks and the modification in the “effective” value of the strange quark chemical potential i.e. μ_s^* in the VDW type approach is less significant as compared to the μ_B^* .

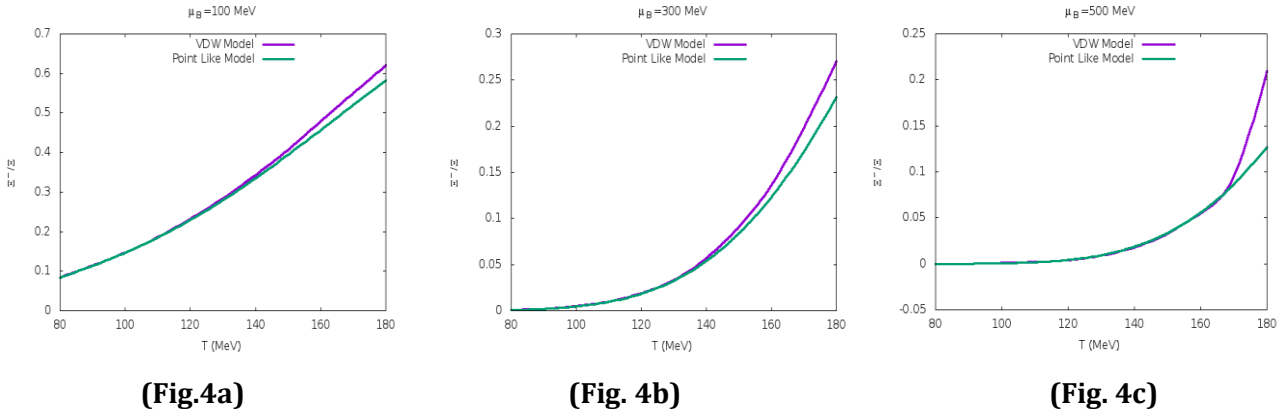


Fig 4: Variation of particle ratios $\left(\frac{\bar{\Xi}}{\bar{\Sigma}}\right)$ with temperature at fixed baryon chemical potential $\mu_B = 100 \text{ MeV}$ (Fig. 4a), 300 MeV (Fig. 4b) and 500 MeV (Fig. 4c).

In figures 5(a) and 5(b), the variation of the triply (anti)strange particle ratio, i.e. $\left(\frac{\bar{\Omega}}{\Omega}\right)$ with temperature at fixed baryon chemical potential $\mu_B = 300 \text{ MeV}$ and 500 MeV . We have compared the ratio $\left(\frac{\bar{\Omega}}{\Omega}\right)$ with the point-like hadron case. Here the situation however becomes interesting. It is found that using van der Waals (VDW) EoS the ratio $\left(\frac{\bar{\Omega}}{\Omega}\right)$ gets suppressed as compared to the point like case. This behaviour is opposite to the previous cases of $\frac{\bar{N}}{N}$, $\frac{\bar{\Lambda}}{\Lambda}$ and $\frac{\bar{\Xi}}{\Xi}$. At lower baryon chemical potentials $\mu_B \leq 100 \text{ MeV}$ the suppression is insignificant.

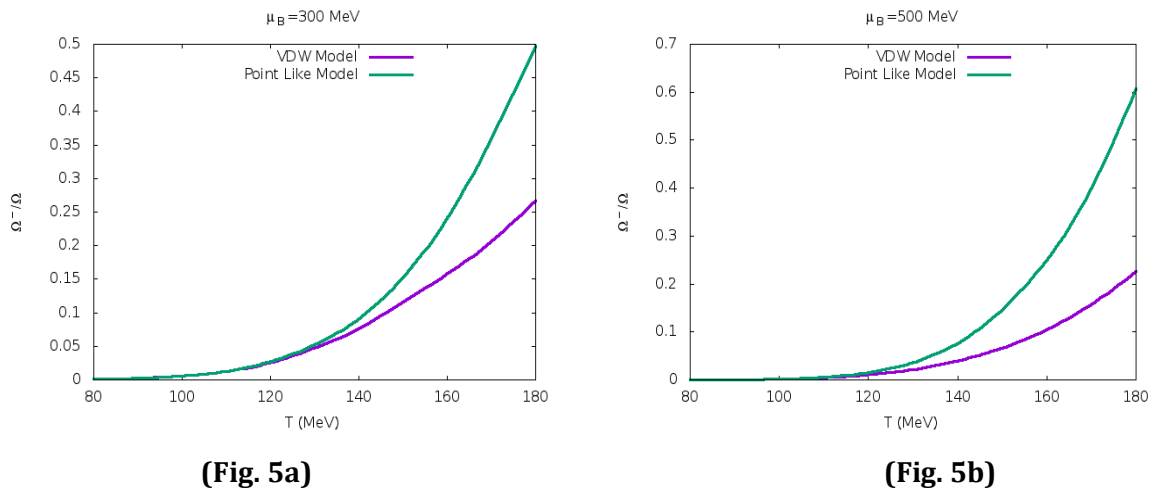


Fig 5: Variation of particle ratio $\left(\frac{\bar{\Omega}}{\Omega}\right)$ with temperature at fixed baryon chemical potential $\mu_B = 300 \text{ MeV}$ (Fig. 5a) and 500 MeV (Fig. 5b).

We have also calculated the strange meson ratios using the VDW type EoS. In figures 6(a), 6(b) and 6(c) we have plotted variation of antikaons to Kaon $\left(\frac{K^-}{K^+}\right)$ ratio with temperature of the system at fixed baryon chemical potential $\mu_B = 100$ MeV, 300 MeV and 500 MeV, respectively. We find that this ratio get appreciably modified as compared to the point like hadron case for temperatures $T > 140$ MeV and shows an increasing pattern at sufficiently higher temperatures and chemical potentials.

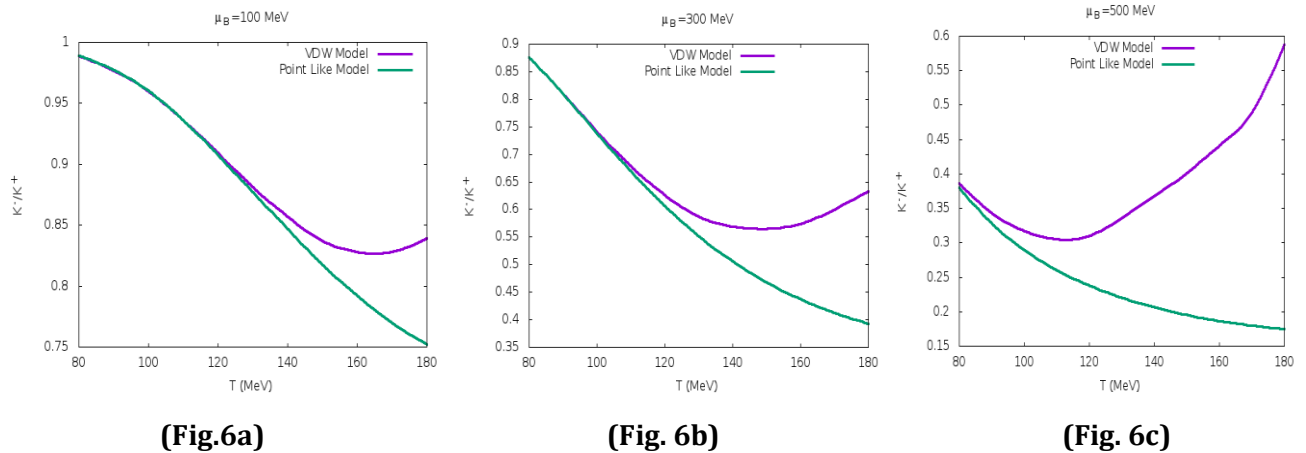


Fig 6: Variation of particle ratio $\left(\frac{K^-}{K^+}\right)$ with temperature at fixed baryon chemical potential $\mu_B = 100$ MeV (Fig. 6a), 300 MeV (Fig. 6b) and 500 MeV (Fig. 6c).

Variation of these particle ratios with baryon chemical potential at different fixed values of temperature is shown in figures 7 and 8.

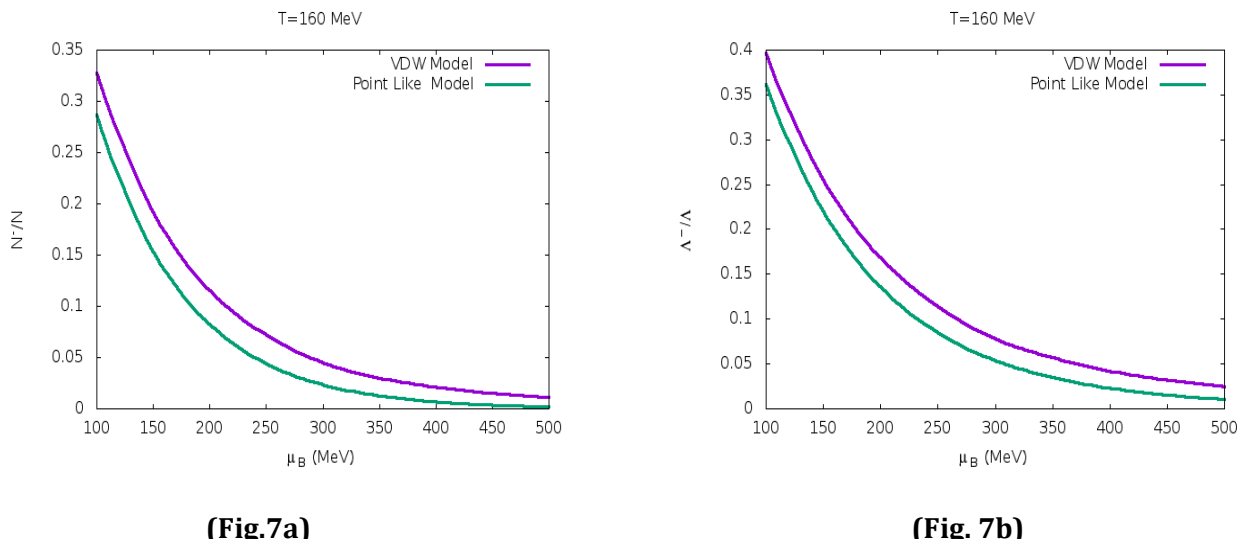
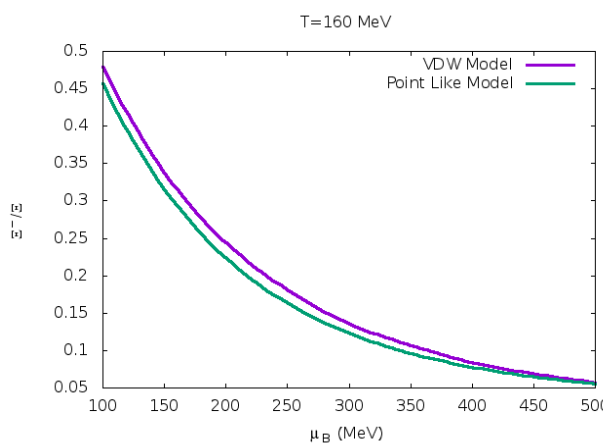
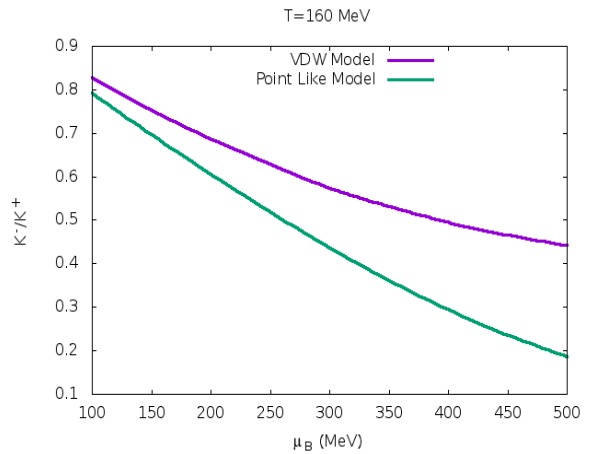


Fig 7: Variation of particle ratios $\left(\frac{\bar{N}}{N}\right)$, (Fig. 7a) and $\left(\frac{\bar{\Lambda}}{\Lambda}\right)$, (Fig. 7b) with baryon chemical potential (μ_B) at fixed temperature $T=160$ MeV.



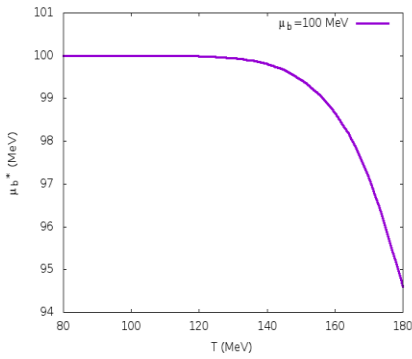
(Fig. 8a)



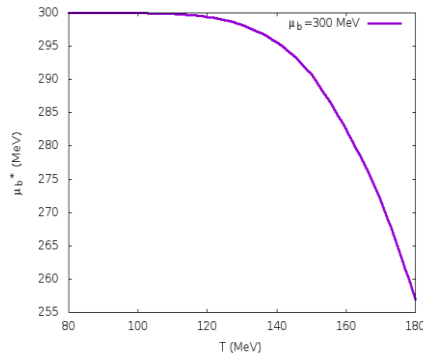
(Fig. 8b)

Fig 8: Variation of particle ratios $\frac{\Xi^-}{\Xi^0}$, (Fig. 8a) and $\frac{K^+}{\bar{K}^0}$, (Fig. 8b) with baryon chemical potential (μ_B) at fixed temperature $T=160$ MeV.

In figures 9(a), 9(b) and 9(c), we have plotted the variation of “effective” baryon chemical potential (μ_B^*) as a function of temperature at fixed values of baryon chemical potential $\mu_B=100$ MeV, 300 MeV and 500 MeV, respectively. We notice that on increasing temperature the “effective” baryon chemical potential (μ_B^*) goes on decreasing, which is more appreciable at higher baryon chemical potential. Further the decrease is appreciable at lower temperatures as μ_B is increased.



(Fig. 9a)



(Fig. 9b)

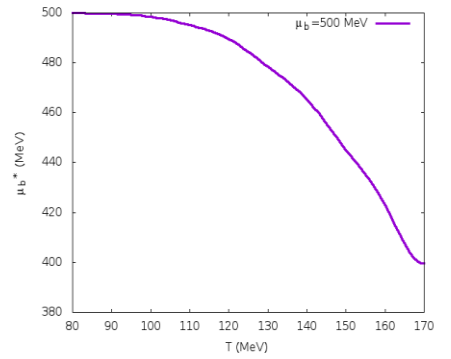


(Fig. 9c)

Fig 9: Variation of effective baryon chemical potential (μ_B^*) at chemical potential $\mu_B = 100$ MeV (Fig. 9a), 300 MeV (Fig. 9b) and 500 MeV (Fig. 9c) as a function of temperature.

In figures 10(a), 10(b) and 10(c), we have plotted the variation of “effective” strange chemical potential (μ_s^*) with the temperature at fixed baryon chemical potentials $\mu_B = 100$ MeV, 300 MeV and 500 MeV, respectively. The μ_s^* value obtained using van der Waals (VDW)

model is compared with the point-like hadron case (i.e. μ_s). We notice that the “effective” strange chemical potential (μ_s^*) get enhanced in van der Waals (VDW) type EoS as compared in point-like hadron case at higher temperatures.

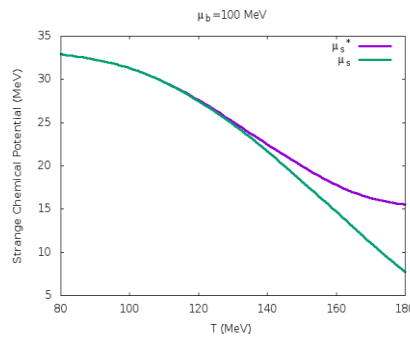


(Fig.10a)

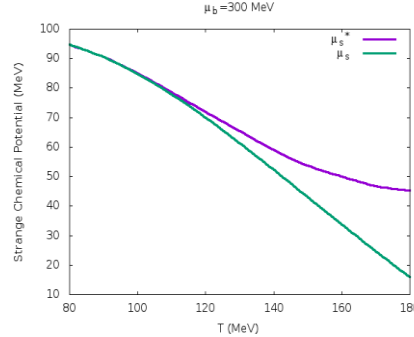


(Fig. 10b)

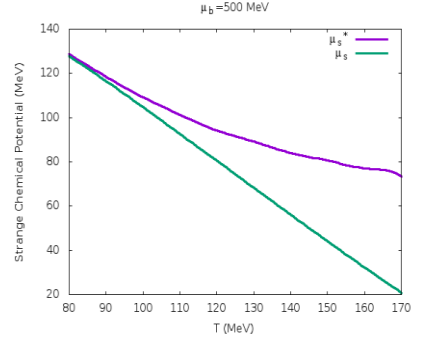


(Fig. 10c)

Fig 10: Variation of “effective” strange chemical potential (μ_s^*) with temperature at fixed baryon chemical potentials $\mu_B = 100$ MeV (Fig. 11a), 300 MeV (Fig. 11b) and 500 MeV (Fig. 11c).

In the figures 11(a) and 11(b), we have shown the dependence of μ_s^* on μ_B at fixed values of temperature, 120 MeV and 160 MeV, respectively. We have compared the “effective” strange chemical potential (μ_s^*) using van der Waals (VDW) type EoS with the point-like hadrons case value (μ_s). The μ_s^* gets modified using van der Waals (VDW) type EoS which becomes significant for larger values of temperature and chemical potential.

Further for the sake of illustration we have in figure 11(c) plotted the variation of the “effective” baryon chemical potential (μ_B^*) with μ_B at various temperatures (T=80 MeV, 120 MeV and 160 MeV). We find that at T and μ_B the μ_s^* shows appreciable suppression.

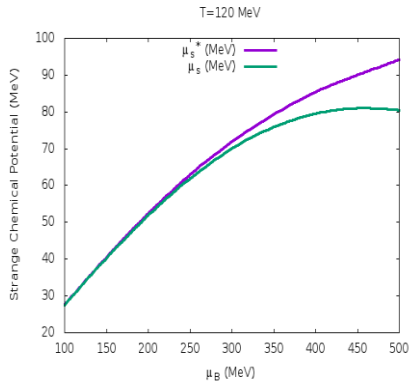


(Fig. 11a)

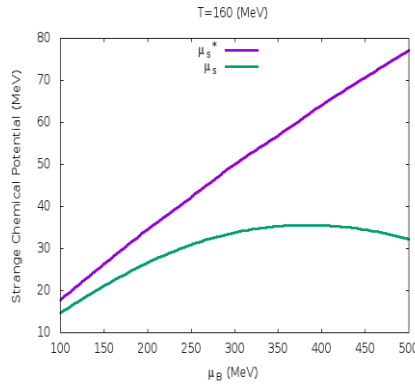


(Fig. 11b)

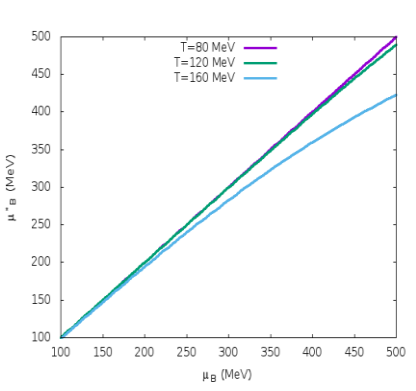


(Fig. 11c)

Fig 11: Variation of “effective” strange (μ_s^*) and “effective” baryon (μ_B^*) chemical potentials with baryon chemical potential (μ_B) at fixed temperatures.

In order to show the dependence of particle ratio on hard core radius value (i.e. repulsive parameter) of (anti)baryon, in figure 12, we have plotted the variation of $\left(\frac{\bar{N}}{N}\right)$ ratio with temperature, at fixed baryon chemical potential ($\mu_B = 100$ MeV, 300 MeV and 500 MeV), using the VDW type EoS for different hard core radii (r_h) of (anti)baryons. It can be easily seen that as the hard-core radii of (anti)baryons become less and less, the value of the ratio thus obtained from the VDW type EoS asymptotically merges with the point-like baryon case. Further we find that at higher temperature, baryon chemical potential (μ_B) and large hard core radii (r_h), the enhancement in $\left(\frac{\bar{N}}{N}\right)$ ratio is large.

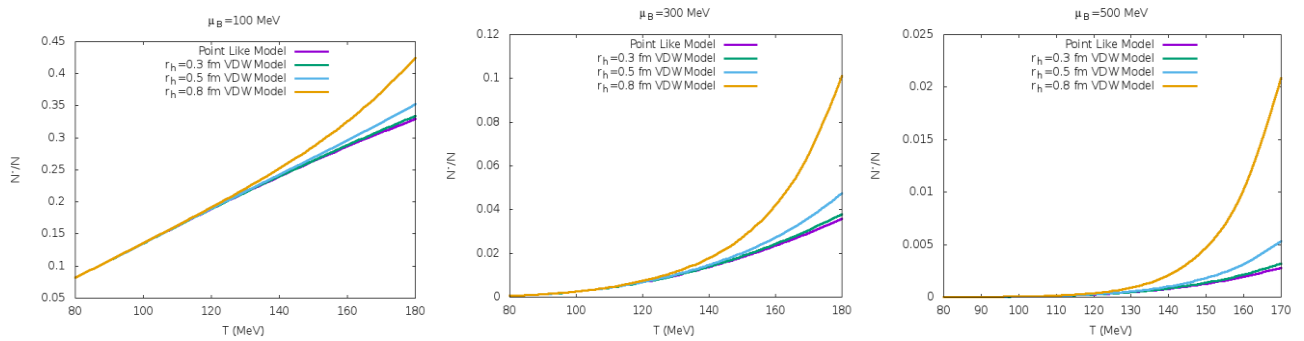


Fig 12: Variation of particle ratios $\left(\frac{\bar{N}}{N}\right)$ with temperature at fixed baryon chemical potentials, $\mu_B = 100$ MeV, 300 MeV and 500 MeV and for different values of hard core radii.

4. Summary and Conclusion:

We have provided a grand canonical ensemble formulation for a multi-component hadron gas. We have considered the attractive as well as repulsive interaction among the constituent particles. The EoS thus obtained is thermodynamically consistent. The attractive parameter a is made temperature dependent in order to restore baryon symmetry in the system at zero baryon chemical potential. Using our formulation we have calculated several particle ratios like $\frac{\bar{N}}{N}$, $\frac{\bar{\Lambda}}{\Lambda}$, $\frac{\bar{\Xi}}{\Xi}$, $\frac{\Omega^+}{\Omega^-}$ & $\frac{K^-}{K^+}$. The variations of the “effective” baryon chemical potential (μ_B^*) and “effective” strange chemical potential (μ_s^*) with T and μ_B have been studied. We find that the particle ratios get modified particularly at higher values of T and μ_B by using the thermodynamically consistent van der Waals type EoS.

Conflicts of Interest

The authors declare that they have no conflicts of interest.

Acknowledgments

Rameez Ahmad Parra is thankful to the Council of Scientific & Industrial Research (CSIR), New Delhi, for providing Junior Research Fellowship.

References

- [1] J. Cleymans, R.V. Gavai, E. Suhonen Phys. Rep. 130 (1986) 217.
- [2] D.H. Rischke et al , Z. Phys. C-Particles and Fields 51, 485-489 (1991).
- [3] Inam-ul Bashir et al., Adv. in HEP, Article ID 9285759 (2018).
- [4] Inam-ul Bashir et al., Adv. in HEP, Article ID 8219567 (2019).
- [5] W. Greiner, L. Neise and H. Stocker Thermodynamics and statistical Mechanics,1995 Springer-Verlag New York, Inc.
- [6] L.D. Landau and E. M. Lifshitz, Statistical Physics (Oxford: Pergamon) 1975.
- [7] Parra et al. Journal of Experimental and Theoretical Physics, 2019, No.2, pp. 217-228.
- [8] Y. Hama, T. Kodama, and O. Socolowski, Braz. J. Phys. 35, 24 (2005).
- [9] K. Werner, Iu. Karpenko, T. Pierog, M. Bleicher and K. Mikhailov, Phys. Rev. C 82 044904 (2010).
- [10] A. V. Merdeev, L. M. Satarov, and I. N. Mishustin, Phys. Rev. C 84, 014907 (2011).
- [11] Saeed Uddin and C.P. Singh, Zeitschrift fur Physics C63, 147-150, (1994).
- [12] J.D. Walecka, Ann. Phys. (N.Y.) 83, 491 (1974).
- [13] B. D. Serot and J. D. Walecka, Int. Journ. Mod. Phys. E 6, 515 (1997).
- [14] W. Bashir, S. Uddin, and R. A. Parra, Nucl. Phys. A 969, 151 (2018).
- [15] D. anchiskin and V. Vovchenko, arXiv:1411.1444v3 [nucl-th] 13 Aug 2015.
- [16] V. Vovchenko, D. V. Anchishkin and M. I. Gorenstein, arXiv:1501.03785v2 [nucl-th] 4 Feb 2015.
- [17] Volodymyr Vovchenko, Mark I. Gorenstein and Horst Stoecker, Eur. Phys. J. A (2018) 54:16.
- [18] Subhasis Samanta and Bedangadas Mohanty, arXiv:1709.04446v2 [hep-ph] 15 Jan 2018.
- [19] Nachiketa Sarkar and Premomoy Ghosh, arXiv:1807.02948v1 [hep-ph] 9 Jul 2018.
- [20] Ranjita K. Mohapatra etal, arXiv:1901.07238v1 [hep-ph] 22 Jan 2019.
- [21] Volodymyr Vovchenko, Mark I. Gorenstein and Horst Stocker PRL 118,182301 (2017).
- [22] R. Venugopalan and M. Prakash, Nucl. Phys. A546, 718 (1992).